Journal of Theoretical and Applied Mechanics, Sofia, Vol.54 (2024) pp. 46-60
INTERDISCIPLINARY TOPICS

DETERMINATION OF THE MODERN SINGLE SHAFT GAS TURBINE ROTOR THERMAL STRESSES

SERHII MORHUN*

Department of Engineering Mechanics and Technology of Machinebuilding, Admiral Makarov National University of Shipbuilding, Mykolaiv, Ukraine

[Received: 8 June 2022. Accepted: 9 March 2023]

doi: https://doi.org/10.55787/jtams.24.54.1.046

ABSTRACT: The paper outlines a finite elements refined mathematical model of the thermal state of modern single shaft gas turbine engine that can be used in ground or floating power plants. The mathematical model is based on special finite elements of hexagonal type. On the base of the developed mathematical model the turbine rotor temperature field was found and experimentally verified. Using the results of temperature field calculation the rotor thermal deformations and stresses have been found too. The obtained results could be used in further studies of the turbine rotor stress-strain state and fatigue strength.

KEY WORDS: Gas turbine rotor, thermal stresses, temperature field, refined mathematical model, finite elements method, experimental verification.

1 INTRODUCTION

In modern conditions of gas turbine engines construction development, the prevailing tendency is increasing the engine's capacity. To ensure the required level of reliability of the developed gas turbine engines, it is necessary to solve a number of problems in different areas, such as fluid flow dynamics, heat transfer, mechanics of solid deformable body etc. On the other hand all of these problems are interconnected, because the results of one problem solution are used as initial data for the other problems solution. Thus for the purpose of the modern single shaft three stages turbine rotor thermal stress-strain state we use the results of the fluid flow analysis for this rotor as initial data [1].

The problem of the gas turbine rotor thermal stress-strain state is rather complex. For its solution we first of all need to solve the problem of heat transfer from gas flow to impellers, forming the turbine rotor.

There are several methods that could be used for the heat transfer study. But in modern literature, the issues of heat transfer from the turbulent fluid or gas flow to

*Corresponding author e-mail: serhii.morhun@nuos.edu.ua

the solid bodies are linked with the finite elements method (FEM) usage. While FEM approximation we also need to take in account that turbine blades are solid bodies with curvilinear surfaces. Thus in the paper [2] not only non-cooled, but also cooled turbine blades models on the base of FEM are given. But the main disadvantage of these models is a description of blades feather by the plane finite elements of triangular type. These circumstances sharply decrease the reliability of the obtained results. To prevent all these disadvantages, in the papers [3–10] the three-dimensional finite element models are used. For example, in [11] special finite elements of shell type were used. In the paper [12] the authors simulate the blade's feather using the eight-node finite elements of prismatic type and in the paper [13] – four-node finite elements of tetrahedron type. In the paper [14] the mathematical model of the steam turbine blade is built on the base of tetrahedron finite elements too. But such type of elements can't correctly describe constructional non-homogeneity of blade's feather, caused by its sharp curvature and especially the form of cooling cavity for the cooled blades.

The paper [15] deals with the research of single crystal turbine blades stress-strain state. In it the processes of the thermal stresses field formation have been studied, but the problem of thermal deformation had not been taken into consideration. The full-scale experimental methods of the external heat transfer used for the fairly accurate determination of the turbine blades temperature field are given in literature [16–18]. However, the process of a full-scale experiment is very expensive, therefore, it is necessary to solve the problem of determining the conditions of external heat transfer at the design stage. It should be also admitted that the vast majority of publications study only the blades thermal state, rejecting the fact that the whole rotor is a unity of solid bodies. That's why the temperature field of the whole rotor is unite too.

Based on the analysis of the above sources, it can be concluded that at the moment there are still a number of unsolved problems regarding the design of highly loaded single shaft GTE rotors through numerical methods. One of them is the turbine rotor temperature field determination. And on its base the rotor thermal stress-strain state more accurately could be obtained. This study would be held using the refined mathematical model on the base of FEM.

2 The Aim and Objectives of Study

The *research object* is the heat exchange between the turbulent working flow and the solid bodies, forming the turbine rotor. The whole rotor should be considered as an assembly of three impellers, connecting together by means of a shaft. Each impeller also is an assembly that consists of the disk and working blades of the same shape and geometric characteristics. The *research subject* is thermal stresses and thermal deformations of the turbine rotor, caused by the heat flux from the turbulent working

flow to the solid bodies.

Thus the aim of the research is to develop a refined mathematical model for calculating the temperature field of the gas turbine rotor and caused by it rotor thermal deformations and thermal stresses.

To achieve this aim, the following tasks must be solved:

- Develop a refined mathematical model for determining the rotor field of temperature on the base of FEM and its experimental verification;
- Determine the temperature fields on the surface of the impellers and the whole rotor;
- Determine the rotor thermal stresses.

3 Formulation of the Problem

3.1 Gas turbine rotor coordinate system

As the stationary coordinate system, the Cartesian right-handed xyz coordinate system with the center at point O located on the gas turbine engine axis is taken. The x axis is perpendicular to the turbine axis, and the z axis coincides with this axis (Fig. 1). The coordinate system rotates together with the rotor at constant angular velocity Ω.

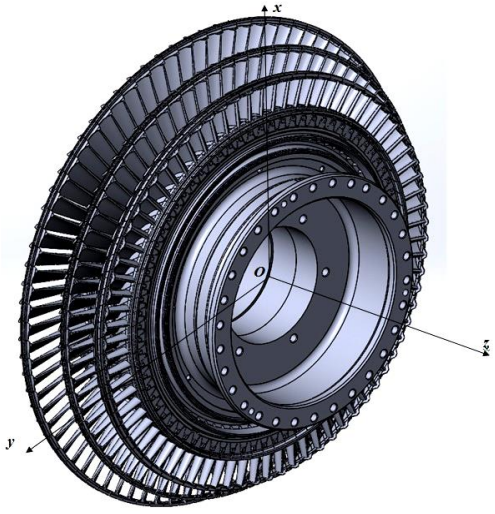

Fig. 1: Gas turbine rotor in the Cartesian right-handed coordinate system.

3.2 Main dependences for the rotor thermal stress-strain state study

The field of the designed gas turbine rotor thermal stresses can be represented by the following matrix equation:

$$\{\sigma_T\} = \left\{ \begin{array}{c} \sigma_{xT} \\ \sigma_{yT} \\ \sigma_{zT} \end{array} \right\} = [D]\ \{\varepsilon_T\}\ , \tag{1}$$

where $\{\sigma_0\|$ is the thermal stresses matrix-vector; σ_{x0}, σ_{y0}, σ_{z0} – the thermal stresses vector projections on the x, y, z coordinate axis; $[D]$ – elasticity matrix of the turbine rotor material; $\{\varepsilon_0\}$ – thermal deformation vector.

The vector of the rotor thermal deformation is represented by eq. (2)

$$\{\varepsilon_T\} = \left\{ \begin{array}{c} \alpha T_x \\ \alpha T_y \\ \alpha T_z \end{array} \right\}, \tag{2}$$

where α – thermal extension coefficient of the rotor material; T_x, T_y, T_z – the rotor temperature field projections on the x, y, z coordinate axis.

Components of the matrix $[D]$ as well as the coefficient α should be taken for the specially developed high-temperature nickel-titanium alloy.

Thus on the base of eq. (1) and eq. (2), we see that solution to the turbine rotor stress-strain state problem depends on the correct finding of the rotor temperature field.

4 Solution to the Problem and Its Experimental Verification

4.1 Mathematical model of the rotor thermal state

The temperature state of the solid body can be described by next variation eq. (3) [19, 20]:

$$\delta J_T = 0\,, \tag{3}$$

where J_T is the thermal functional.

For the functional J_T minimization we need to use the general heat equation

$$\lambda_x \frac{\partial^2 T}{\partial x^2} + \lambda_y \frac{\partial^2 T}{\partial y^2} + \lambda_z \frac{\partial^2 T}{\partial z^2} = 0\,, \tag{4}$$

where λ_x, λ_y, λ_z are the thermal conductivity coefficients on the x, y, z coordinate axis, [W/(mK)].

As the heat exchange between the gas flow and the rotor surfaces is convective the boundary conditions for eq. (4) are represented by eq. (5)

$$\lambda_x \frac{\partial T}{\partial x} l_x + \lambda_y \frac{\partial T}{\partial y} l_y + \lambda_z \frac{\partial T}{\partial z} l_z + h\,(T - T_0) - q = 0\,, \tag{5}$$

where l_x, l_y, l_z denote direction cosines; h – heat transfer coefficient, [W/m^2/K]; T_0 – gas flow temperature, [K]; q – heat flux density, [W/m^2].

Using eqs. (4) and (5), the variation eq. (3) can be given in the next form [21]:

$$\begin{aligned} J_T = & \frac{1}{2} \int\limits_V \left[\lambda_x \Big(\frac{\partial T}{\partial x} \Big)^2 + \lambda_y \Big(\frac{\partial T}{\partial y} \Big)^2 + \lambda_z \Big(\frac{\partial T}{\partial z} \Big)^2 \right] dV \\ & + \int\limits_S \left[\frac{1}{2} h (T - T_0)^2 - qT \right] dS\,, \end{aligned} \tag{6}$$

where V is the turbine rotor volume; S – square of the heat exchanging surfaces.

Analytical solution of eq. (6) for the case of convective heat transfer from turbulent gas flow to the solid body does not exist. Therefore, it is necessary to use numerical methods, namely, the finite elements method.

4.2 FEM APPROXIMATION OF THE TURBINE ROTOR MODEL

For the FEM approximation the rotor solid body continuum should be replaced by a discrete area, formed by unity of finite elements. So the minimization of the functional J_T takes place on the set of finite elements model nodes. The process of functional J_T minimization starts by introducing several matrixes

$$\{H_T\} = \left\{ \begin{array}{c} \partial T/\partial x \\ \partial T/\partial y \\ \partial T/\partial z \end{array} \right\}, \qquad [D_T] = \left[\begin{array}{ccc} \lambda_x & 0 & 0 \\ 0 & \lambda_y & 0 \\ 0 & 0 & \lambda_z \end{array} \right], \tag{7}$$

where H_T denotes the matrix of the first derivatives of the turbine rotor temperature field on the Cartesian coordinate system axis x, y, z; D_T – matrix of thermal conductivity coefficients.

Using eq. (7), eq. (6) can be transformed

$$J_T = \frac{1}{2} \int\limits_V \{H_T\}^T [D_T] \{H_T\}\, dV + \frac{1}{2} \int\limits_S \left[h\,(T - T_0)^2\, dS \right] - \int\limits_S qT dS\,. \tag{8}$$

As the temperature function is not discontinuous over the entire definition dominion it is necessary to take into consideration functions T_e that are defined and

continuous on each finite element. Thus on the base of eq. (8) the thermal functional of each finite element is given

$$J_{Te} = \frac{1}{2}\int\limits_{V_e} \{H_{Te}\}^T [D_T] \{H_{Te}\}\, dV_e + \frac{1}{2}\int\limits_{S_e} \left[h\,(Te - T_0 e)^2\, dS_e\right] - \int\limits_{S_e} q_e T_e dS_e\,, \quad e = 1\ldots., m\,. \tag{9}$$

So the whole rotor thermal functional J_T can be presented in the next form:

$$J_T = \sum_{e=1}^{m} J_{Te}\,, \tag{10}$$

where m marks the quantity of finite elements approximating the turbine rotor model.

Interpolation polynomial approximating the temperature of the finite element is represented as

$$T_e = [N]\{T\} = \left[\begin{array}{cccc} N_1 & N_2 & \cdots & N_n \end{array}\right] \left\{\begin{array}{c} T_1 \\ T_2 \\ \vdots \\ T_n \end{array}\right\}, \tag{11}$$

where $[N]$ is the finite element shape functions matrix; n – number of the finite element nodes.

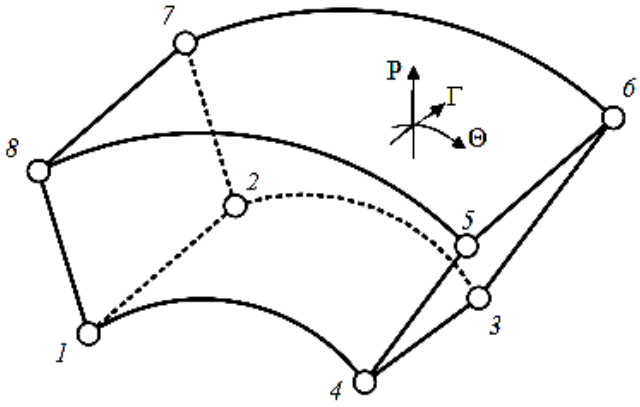

Fig. 2: Hexagonal finite element and its local curvilinear coordinate system P Γ Θ.

According to the gas turbine blades and disks geometry, the turbine rotor should be considered as a space solid body, with the surfaces of complicated curvilinear form. Thus for its correct finite elements approximation we use curvilinear finite elements of hexagonal type (Fig. 2).

Finite element shape functions, forming the matrix $[N]$ in eq. (11) are given below:

$$
\begin{aligned}
N_1 &= \frac{1}{8}(1-\Theta)(1-\mathrm{P})(1-\Gamma)\,, & N_2 &= \frac{1}{8}(1-\Theta)(1-\mathrm{P})(1+\Gamma)\,,\\
N_3 &= \frac{1}{8}(1+\Theta)(1-\mathrm{P})(1+\Gamma)\,, & N_4 &= \frac{1}{8}(1+\Theta)(1-\mathrm{P})(1-\Gamma)\,,\\
N_5 &= \frac{1}{8}(1+\Theta)(1+\mathrm{P})(1-\Gamma)\,, & N_6 &= \frac{1}{8}(1+\Theta)(1+\mathrm{P})(1+\Gamma)\,,\\
N_7 &= \frac{1}{8}(1-\Theta)(1+\mathrm{P})(1+\Gamma)\,, & N_8 &= \frac{1}{8}(1-\Theta)(1+\mathrm{P})(1+\Gamma)\,.
\end{aligned}
\tag{12}
$$

Using the element shape functions from eq. (12), we form the coordinate transformation between the global coordinate system of rotor and local coordinate system of finite element

$$
\begin{Bmatrix} x \\ y \\ z \end{Bmatrix} = \sum_{i=1}^{8} N_i\left(\Theta, \mathrm{P}, \Gamma\right) \begin{Bmatrix} x_i \\ y_i \\ z_i \end{Bmatrix}. \tag{13}
$$

Then for the each finite element matrix H_{Te} will be formed on the base of eqs. (11)–(13)

$$
\begin{aligned}
\{H_{Te}\} &= \begin{Bmatrix} \dfrac{\partial T_e}{\partial x} \\ \dfrac{\partial T_e}{\partial y} \\ \dfrac{\partial T_e}{\partial z} \end{Bmatrix} = \begin{bmatrix} \dfrac{\partial N_1}{\partial x} & \dfrac{\partial N_2}{\partial x} & \cdots & \dfrac{\partial N_8}{\partial x} \\ \dfrac{\partial N_1}{\partial y} & \dfrac{\partial N_2}{\partial y} & \cdots & \dfrac{\partial N_8}{\partial y} \\ \dfrac{\partial N_1}{\partial z} & \dfrac{\partial N_2}{\partial z} & \cdots & \dfrac{\partial N_8}{\partial z} \end{bmatrix} \begin{Bmatrix} T_1 \\ T_2 \\ \vdots \\ T_8 \end{Bmatrix} \\
&= [B_T]\,\{T\}\,, \qquad e = 1, \ldots, m\,,
\end{aligned}
\tag{14}
$$

where B_T – matrix of gradients.

As temperature is a scalar value the matrix of gradients for each finite element node has 3x3 dimension. So for our finite element it looks like

$$
[B_{Ti}] = \begin{bmatrix} \partial N_i/\partial x & 0 & 0 \\ 0 & \partial N_i/\partial y & 0 \\ 0 & 0 & \partial N_i/\partial z \end{bmatrix}, \qquad i = 1, \ldots, 8\,. \tag{15}
$$

Thus on the base of eqs. (11)–(15) the thermal functional for each finite element can be performed like this

$$J_{Te} = \frac{1}{2}\int\limits_{V_e} \{T\}^T [B_{Te}][D_T][B_T]\{T\} dV_e + \frac{1}{2}\int\limits_{S_e} h\{T\}^T [N_e]^T [N_e\{T\}] dS_e - \int\limits_{S_e} hT_0 \left[N_e\right]\{T\}\, dS_e + \frac{1}{2}\int\limits_{S_e} T_0^2 dS_e - \int\limits_{S_e} q\left[N_e\right]\{T\}\, dS_e\,, \quad e = 1, \ldots, m\,. \tag{16}$$

Differentiating the functional in eq. (16) by the temperature of the finite element, we receive next dependencies for the functional constituents:

$$\begin{aligned}
&\frac{\partial}{\partial\{T\}}\int\limits_{V_e} \frac{1}{2}\{T\}^T [B_{Te}]^T [D_T][B_T]\{T\} dV_e = \int\limits_{V_e} [B_{Te}][D_T][B_T]\{T\} dV_e\,,\\
&\frac{\partial}{\partial\{T\}}\int\limits_{S_e} \frac{1}{2} h\{T\}^T [N_e]^T [N_e]\{T\} dS_e = \int\limits_{S_e} h[N_e]^T [N_e]\{T\} dS_e\\
&\frac{\partial}{\partial\{T\}}\int\limits_{S_e} hT_0\left[N_e\right]\{T\}\, dS_e = \int\limits_{S_e} hT_0\left[N_e\right]^T dS_e\,,\\
&\frac{\partial}{\partial\{T\}}\int\limits_{S_e} \frac{1}{2} hT_0^2 dS_e = 0\,,\\
&\frac{\partial}{\partial\{T\}}\int\limits_{S_e} q\left[N_e\right]\{T\}\, dS_e = \int\limits_{S_e} q\left[N_e\right]^T dS_e\,.
\end{aligned} \tag{17}$$

Thus on the base of eq. (17), we receive

$$\frac{\partial J_{Te}}{\partial\{T\}} = \left(\int\limits_{V_e} [B_{Te}]\,[D_T]\,[B_T]\, dV_e + \int\limits_{S_e} h\left[N_e\right]^T [N_e]\{T\}\, dS_e\right)\{T\} - \int\limits_{S_e} hT_0\left[N_e\right]^T dS_e - \int\limits_{S_e} q\left[N_e\right]^T dS_e\,, \tag{18}$$

or in the form of matrix equation

$$\frac{\partial J_{Te}}{\partial\{T\}} = [k_{Te}]\{T\} + \{f_{Te}\}\,, \tag{19}$$

where $[k_{Te}]$ – matrix of the finite element thermal conductivity; f_{Te} – vector of the heat exchange between gas flow and the finite element.

Substituting eq. (19) into eq. (9) and taking into consideration eq. (3) and eq. (10), we receive global matrix equation of the whole turbine rotor thermal state

$$\frac{\partial J_T}{\partial \{T\}} = \sum_{e=1}^{m} [k_{Te}] \{T\} + \{f_{Te}\}$$

or

$$[K_T] \{T\} = \{F_T\}, \tag{20}$$

where $[K_T]$ is the global matrix of the turbine rotor thermal conductivity; $\{T\}$ – vector of the turbine rotor temperature; $\{F_T\}$ – vector of the heat exchange between the turbine rotor and gas flow.

Solution of eq. (20) gives an opportunity to find the turbine rotor temperature vector that was needed for use in eq. (2) and eq. (1) for the solution of turbine rotor thermal stress-strain state problem.

4.3 Experimental Verification of the Developed Mathematical Model

For the verification of the developed refined mathematical model an experimental investigation has been held. On the average section surface of the most heated blades of the first impeller the special temperature sensors have been mounted. The digital

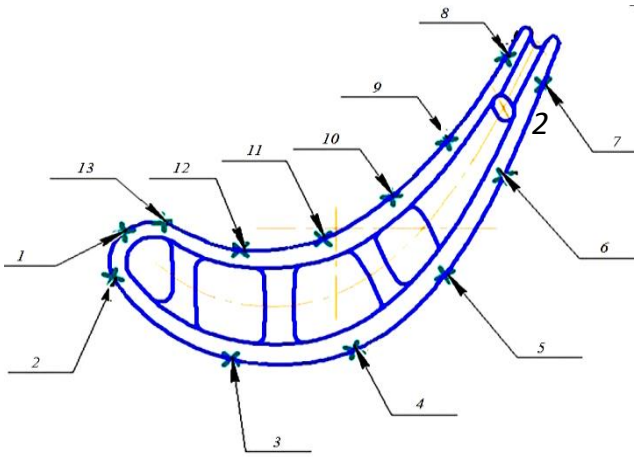

Fig. 3: The scheme of the thermal sensors location on the blade average section surface.

data from sensors have been transmitted to a special decoder and compared with the calculated results. The scheme of sensors location on the blades average section surface is given in Fig. 3. Experiment has been carried out with a steady air flow that corresponds with the real conditions of the turbine rotor working process as a part of a GTE. The thermal processes in rotor during the turbine start have not been taken into account.

Air temperature during the experiment varies from 1096°C to 1120°C. As the first impeller working blades are cooled the temperature of cooling air at the entrance to the blade cavity varies from 395°C to 410°C.

The results of the blade temperature experimental and numerical definition in the places of sensors location are given in Table 1.

Table 1: First impeller average section blade surface temperature, °C

Sensor's number	Numerical result, °C	Experimental result, °C	Divergence, %
1	1096.328	995.71	9.18
2	1063.469	994.35	6.49
3	983.70	937.46	4.70
4	953.943	904.35	5.20
5	943.219	885.96	6.01
6	973.154	932.28	4.20
7	1037.627	976.09	5.93
8	1074.548	1033.61	3.81
9	1015.316	974.50	4.02
10	996.152	958.09	3.82
11	1013.847	971,36	4,19
12	1042.963	1001.56	3.97
13	1078.284	999.68	7.29

Comparison of the data in Table 1 shows that divergence between numerical and experimental temperatures doesn't exceed 10%. It means that the developed mathematical model is adequate and accurate, and it correctly predicts fields of temperature of the turbine rotor.

5 Results and Discussion

The power of the turbine under study P is 15 MW, the temperature of the working flow at the turbine flow path entrance is 1138°C, the rotor angular velocity Ω is 11330 rev/min.

5.1 THERMAL STATE OF THE TURBINE ROTOR

The results of the developed GTE rotor thermal state analysis are given below in Fig. 4. The impellers and represented in form of sections, containing one blade and a disk sector.

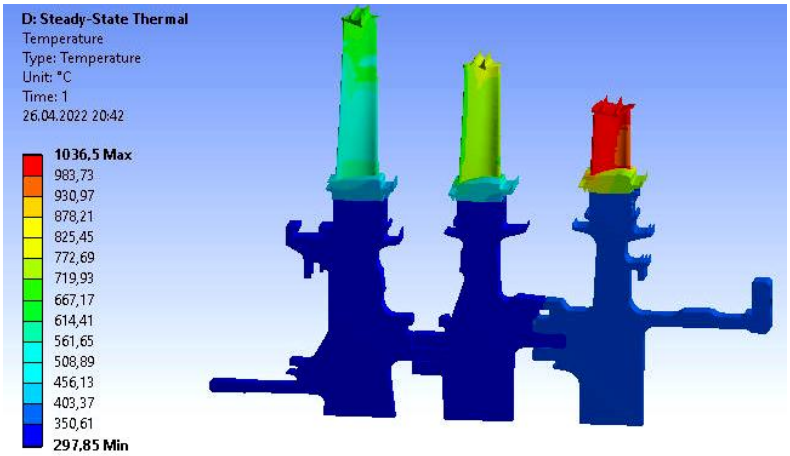

Fig. 4: Thermal state of the turbine rotor section.

Analyzing the data, presented in Fig. 4, we can find a sharp temperature gradient between the disk and the blade. The matter is that the gas flow firstly penetrates the peripheral sections of blades. Thus their temperature is the highest. After that the heat flow expands to the blade root section and only after it starts the heat exchange between the blade and disk.

On the other hand we can see a temperature gradient in a rotor meridian cross-section too. Explanation for this fact is that due to the heat exchange between the gas flow and solid bodies of blades and disks every following impeller receives less quantity of heat than the previous impeller. Thus the temperature of every following impeller is lower than the previous.

Such thermal gradients cause the thermal deformations and form the fields of thermal stresses of each impeller and the whole rotor.

5.2 THERMAL DEFORMATIONS AND THERMAL STRESSES OF THE TURBINE ROTOR

As it was found the temperature gradients are in the rotor meridian and transverse section. So to show correctly the fields of thermal deformations and stresses we will show them in three coordinate directions. These results are given in Figs. 5–7.

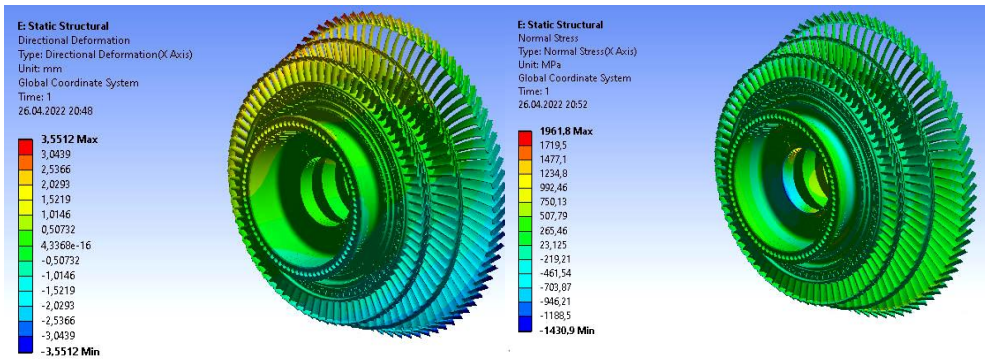

(a) (b)

Fig. 5: Turbine rotor thermal deformations (a) and thermal stresses (b) in the x axis direction.

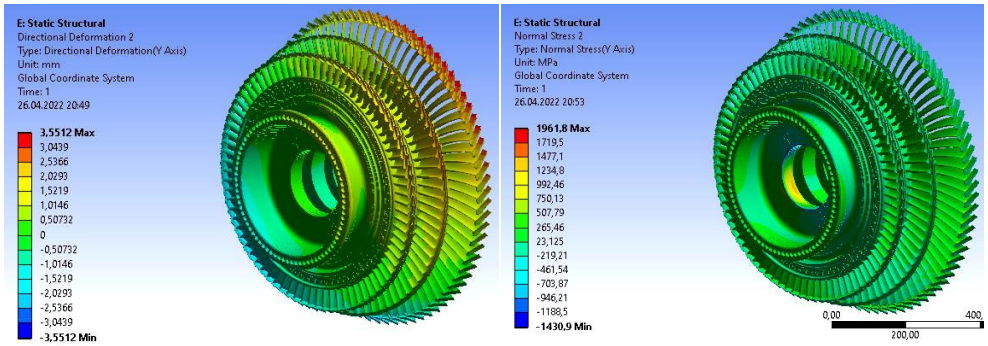

(a) (b)

Fig. 6: Turbine rotor thermal deformations (a) and thermal stresses (b) in the y axis direction.

Analyzing data represented in Figs. 5–7, we can see that the highest thermal deformations are in the x and y coordinate axis directions. This fact agrees well with Fig. 4, where the temperature gradient in the rotor meridian section is shown. Deformation in z axis direction is much less in comparison with x direction and increases from the first impeller to the third. It can be explained by taking in consideration the rotor rotation that causes centrifugal force. Thus the third impeller blades according to their geometric characteristics are more malleable than the first impeller blades.

Normal stresses, caused by the influence of heat flux and centrifugal force are much bigger in the xy plane than in z axis direction. They are caused by a sharp temperature gradients between the blade and the disk for each impeller (Fig. 4). Fur-

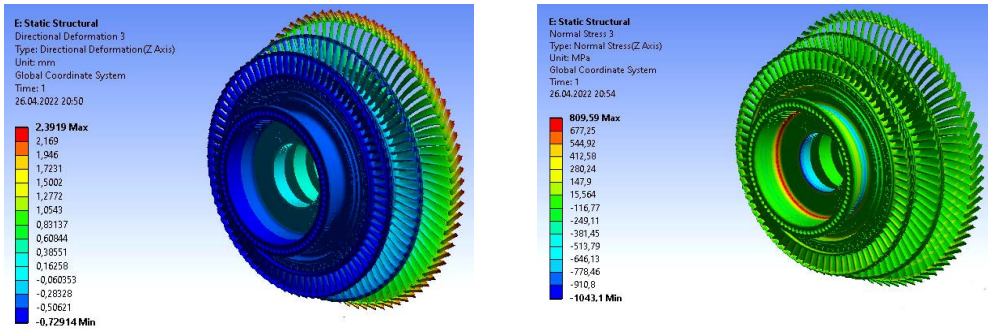

(a) (b)

Fig. 7: Turbine rotor thermal deformations (a) and thermal stresses (b) in the z axis direction.

ther more the drop of thermal stresses is present even between the different parts of the blade, because the blade feather peripheral part is hot up more than the blade root part.

6 Conclusions

The study of the modern single shaft gas turbine rotor thermal state has been held. To solve the aforementioned problem a refined mathematical model based on the hexagonal finite element usage was developed. The reliability and adequacy of this mathematical model are confirmed by experimental data. Using the developed mathematical model and the calculated field of temperature the rotor thermal stress-strain state has been studied too. It has been shown that the highest tensile stresses are in x direction. They are caused not only by the sharp temperature gradient between the peripheral part of the blade, its root part and the disk, but by the influence of centrifugal force too.

All the obtained results together with the data given in [1] would be used for the further studies of the modern GTE rotor forced vibration, stress-strain state and fatigue strength.

References

[1] S. Morhun, S. Vilkul (2022) Gas dynamic analysis of the modern single shaft gas turbine engine flow path. *International Journal of Turbo and Jet Engines*.

[2] S. Wang, L. Shouzuo, L. Lei, Zh. Zhao, D. Wei, S. Bengt (2021) A high temperature turbine blade heat transfer multilevel design platform. *Numerical Heat Transfer, Part A: Applications* **79**(2) 122-145.

[3] L. Luo, C.L. Wang, B. Sunden, S.T. Wang (2016) Heat transfer and friction factor

performance in a pin fin wedge duct with different dimple arrangements. *Numerical Heat Transfer, Part A: Applications* **69**(2) 209-226.

[4] L. LUO, D. QIU, W. DU, B. SUNDEN, ZH. WANG, X. ZHANG (2018) Surface temperature reduction by using dimples/protrusions in a realistic turbine blade trailing edge. *Numerical Heat Transfer, Part A: Applications* **74**(5) 1265-1283.

[5] R. DAS, B. KUNDU (2017) Prediction of heat generation in a porous fin from surface temperature. *Journal of Thermophysics and Heat Transfer* **31**(4) 781-790.

[6] M.R. REIHANI, M. ALIZADEH, A. FATHI, H. KHALEDI (2013) Turbine blade temperature calculation and life estimation – a sensitivity analysis. *Propulsion and Power Research* **2**(2) 148-161.

[7] I. SHEVCHENKO, N. ROGALEV, A. ROGALEV, A. VEGERA, N. BYCHKOV (2018) Verification of thermal models of internally cooled gas turbine blades. *Advances in Fluid Dynamics of Turbomachinery 2018*.

[8] T. SADOWSKI, D. PIETRAS (2016) Heat transfer process in jet turbine blade with functionally graded thermal barrier coating. *Solid State Phenomena* **254** 170-175.

[9] B.P.V.S. MUKHERJI, K. RAJA, G. NARESH, V.N.B. RAO, I.N.N. KUMAR (2015) An investigation of transient thermal analysis of 1^{st} stage gas turbine blade manufactured by directional solidification and mechanically alloyed nickel-based superalloys. *International Journal of Advanced Science and Technology* **85** 17-28.

[10] P. SINGH, O.P. SHUKLA (2020) Heat transfer analysis of gas turbine rotor blade through staggered holes using CFD. *International Journal of Engineering Research and General Science* **4**(2) 263-271.

[11] S. MISURA, N. SMETANKINA, I. MISURA (2020) Optimal design of the cyclically symmetrical structure under the static load. *Integrated Computer Technologies in Mechanical Engineering* **188** 256-266.

[12] L. LUO, C. WANG, L. WANG, B. SUNDEN, S.T. WANG (2016) Endwall heat transfer and aerodynamic performance of bowed outlet guide vans with on- and off-design conditions. *Numerical Heat Transfer, Part A: Applications* **69**(4) 352-368.

[13] K. SINGH, R. DAS, B. KUNDU (2016) Approximate analytical method for porous stepped fins with temperature-dependent heat transfer parameters. *Journal of Thermophysics and Heat Transfer* **30**(3) 661-672.

[14] L. YANG, J. REN, J. HONGDE, Y. LUAN, P. LIGRANI (2015) Assessment of six turbulence models for modeling and predicting narrow passage flows. Part 1: impingement jets. *Numerical Heat Transfer, Part A: Applications* **69**(5) 109-127.

[15] W.T. SU, M. BINAMA, Y. LI, Y. ZHAO (2020) Study on the method of reducing the pressure fluctuation of hydraulic turbine by optimizing the draft tube pressure distribution. *Renewable Energy* **162** 550-560.

[16] L. YANG, J. REN, H. JIANG, Y. LUAN, P. LIGRANI (2014) Experimental and numerical investigation of unsteady impingement cooling within a blade leading edge passage. *International Journal of Heat and Mass Transfer* **71** 57-68.

[17] L. FURLANI, A ARMELLINI, L. CASARSA (2016) Rotational effects on the flow field inside a leading edge impingement cooling passage. *Experimental Thermal and Fluid Science* **76** 57-66.

[18] M.E. TASLIM, A. NONGSAENG (2011) Experimental and numerical cross-over jet impingement in an airfoil trailing edge cooling channel. *Journal of Turbomachinery* **133**(4) 1-10.

[19] K.H. BRAHMAIAH, M.L. KUMAR (2014) Heat transfer analysis of gas turbine blade through cooling holes. *International Journal of Computational Engineering Research* **04**(7) 2250-3005.

[20] S.V. YERSHOV, V.A. YAKOVLEV (2021) The influence of mesh resolution on 3D RANS flow simulations in turbomachinery flow path. *Journal of Mechanical Engineering* **24**(1) 13-27.

[21] S. MORHUN (2022) Numerical analysis of the gas turbine rotor blades thermal state using a refined mathematical model. *Lecture Notes in Networks and Systems* **344** 115-123.